HHS Public Access

Author manuscript

Nanomedicine. Author manuscript; available in PMC 2020 August 01.

Published in final edited form as:

Nanomedicine. 2019 August ; 20: 102025. doi:10.1016/j.nano.2019.102025.

Development of Medical-Grade, Discrete, Multi-walled Carbon Nanotubes as Drug Delivery Molecules to Enhance the Treatment of Hematological Malignancies

Carolyne Falank[1,2], **Aaron W. Tasset**[3], **Mariah Farrell**[1,2], **Sophie Harris**[1,2], **Paul Everill**[3], **Milos Marinkovic**[3], **Michaela R. Reagan**[1,2,4]

[1]Maine Medical Center Research Institute, Scarborough, ME, 04074

[2]Graduate School of Biomedical Science and Engineering, University of Maine, Orono, ME 04469

[3]BioPact LLC, 13477 Fitzhugh Road, Austin, TX, 78736

[4]Tufts University School of Medicine and Sackler School of Biomedical Sciences, Boston, MA, 02111

Abstract

Carbon nanotubes (CNTs) hold great potential as drug delivery transporters given their large drug-binding surface area. Herein, we designed novel, multi-walled, discrete CNTs (dMWCNTs), PEGylated dMWCNTs (PEG-dMWCNTs), and bone-targeting (BT), alendronate-conjugated PEG-dMWCNTs (BT-PEG-dMWCNTs). Using zeta potential, thermogravimetric analysis, TEM, SEM, and FTIR, dMWCNTs were characterized as individual, uniform, and stable. Drug binding and release assays validated dMWCNTs as effective doxorubicin (DOX) transporters. The mass ratio of DOX loading onto dMWCNTs was 35% wt/wt with a ~95% wt/wt efficiency. DOX release was ~51% w/w after 48 hours. Neoplastic transformation, chromosomal aberration, and cytotoxicity assays, confirmed biocompatibility for all dMWCNTs. PEG-dMWCNTs were well tolerated and modulated drug pharmacokinetics in mice. In mice with Burkitt's lymphoma, DOX-loaded PEG-dMWCNTs and BT-PEG-dMWCNTs reduced tumor burden and increased survival similarly to free drug. Importantly, DOX toxicity was abrogated when DOX was loaded onto PEG-dMWCNTs or BT-PEG-dMWCNTs. Overall, PEG-dMWCNTs and BT-PEG-dMWCNTs represent a promising new nanocarrier platform.

Graphical Abstract

Carbon nanotubes (CNTs) hold great potential as drug delivery transporters given their large drug-binding surface area. Herein, we designed novel, discrete, multi-walled CNTs (dMWCNTs), PEGylated dMWCNTs (PEG-dMWCNTs), and bone-targeting (BT), alendronate-conjugated

Corresponding Author and person to whom reprint requests should be addressed: Michaela R. Reagan, PhD, Center for Molecular Medicine and Center for Translational Research, 81 Research Drive, Scarborough, Maine. USA 04074, Phone: 1-207-396-8196, Fax: 1-207-396-8110, Mreagan@mmc.org.

PEG-dMWCNTs (BT-PEG-dMWCNTs). Using zeta potential, thermogravimetric analysis, transmission electron microscopy, scanning electron microscopy, and FTIR, dMWCNTs were characterized as individual, uniform, and stable. Drug binding and drug release assays validated PEG-dMWCNTs and BT-PEG-dMWCNTs as effective doxorubicin (DOX) transporters with pharmacokinetic modulation potential. *In vitro*, biocompatibility was confirmed with neoplastic transformation, chromosomal aberration and cytotoxicity assays for all dMWCNTs. *In vivo*, PEG-dMWCNTs demonstrated systemic tolerability and the ability to modulate drug pharmacokinetics. Lastly, in a Burkitt's lymphoma mouse model, DOX-loaded PEG-dMWCNTs and BT-PEG-dMWCNTs reduced tumor burden and increased survival similarly to free drug. Importantly, DOX toxicity (weight loss) was abrogated when DOX was loaded onto PEG-dMWCNTs or BT-PEG-dMWCNTs. In sum, PEG-dMWCNTs and BT-PEG-dMWCNTs represent a promising new nanocarrier platform.

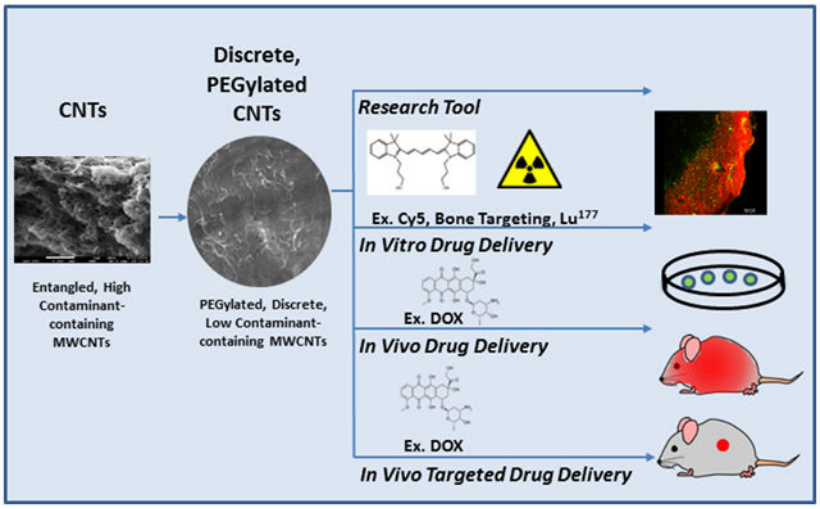

Keywords

Discrete Carbon Nanotubes; Multiwalled Carbon Nanotubes; Burkitt's Lymphoma; Nanomedicine; Drug Delivery

Background

Since the first characterization of carbon nanotubes (CNTs)s ~30 years ago, the development of CNT technology for biomedical applications has grown exponentially, paralleling technological, medical, and computational advances [1]. CNTs are submicron-scale, cylindrical, carbon allotropes that have unique physicochemical characteristics that endow them with great strength, flexibility, molecule-adsorptive surface area, and electrical properties. Due to issues in dispersion uniformity, availability of individual tubes rather than typical bundles, and the potential for toxicity, commercial biomedical applications of CNTs have been limited [2]. Preliminary work focusing on tissue engineering [3], prosthetics [4], bio-imaging [5], drug delivery [6,7], and neuroscience applications [8] has demonstrated the great biomedical potential for CNTs, if aggregation, stability, loading, targeting, imaging, and safety challenges can be overcome [9-11].

Over the last decade, a variety of CNTs have been examined in preclinical oncology studies, but none have entered the clinic. Ali-Boucetta et al. demonstrated the utility of multi-walled CNTs (MWCNTs) loaded with doxorubicin (DOX) *in vitro* [12]. Zhang et al. produced DOX-loaded single-walled CNTs (SWCNTs), directed these towards HeLa cells using folic acid targeting groups, and demonstrated that these had higher killing efficiency than free DOX *in vitro* [13]. SWCNTs coupled to antibodies, such as anti-CD20 and anti-CD22, have demonstrated targeting towards specific cancer cells [14,15]. However, in myeloma, SWCNT-bound daunorubicin had lower efficacy than the drug alone *in vitro*, which impeded further *in vivo* development and highlights the functional disparity between CNT types [16]. A wide array of CNT-drug conjugates have been tested *in vitro* for treatment of cancers including breast, colon, and cervical [17-20]. Transitioning from *in vitro* to *in vivo* has proven to be a major hurdle for multiple reasons and led to a demand for a specifically designed, safe, and efficacious discrete CNT to enable their translation into the clinic.

During mass production, CNT molecules often entangle as macroscopic clumps, frequently larger than 100 μm in diameter, because of Van der Waals attraction [21]. Instead of the discrete “drinking straw” conformation, mass-produced CNTs more closely resemble “balls of yarn” consisting of thousands of aggregated tubes that retain the original metallic catalysts used in their production and frequently present toxic qualities [22]. BioPact™ has licensed a method to produce discrete, MWCNTs, void of aggregative properties, which greatly enhances their efficacy in industrial applications such as energy storage [23,24] and rubber composites [25,26]. For medical applications, we explored here if further processing and PEGylation of dMWCNTs could enhance their biocompatibility and utility for drug delivery. We then loaded the resulting dMWCNTs with drugs and bone targeting moieties, with the goal of developing a new technology that could be used to deliver agents safely *in vitro* and *in vivo*.

Methods

A detailed overview of materials and methods can be found in the Supplementary Data.

Results

Development and Characterization of dMWCNTs

In a preliminary toxicity study, we first validated the hypothesis that discrete MWCNTs were safer than bulk MWCNTs. To do this, we planned to injected 500 μg bulk CNTs or dMWCNTs (i.v., tail vein) to mice (male CD-1 mice aged 6-8 weeks) every three days for 18 days. However, the bulk MWCNTs killed all the mice in the group on the first day. The mice with dMWCNTs continued in the experiment until the end and appeared healthy and unaffected at the end of the toxicity study. This finding demonstrated that bulk MWCNTs would not be safe *in vivo* and would need to be modified for drug delivery applications.

We then designed two distinct formulations of multiwalled, discrete carbon nanotubes (dMWCNTs) and pegylated dMWCNTs (PEG-dMWCNTs)) and compared these to the bulk, unprocessed MWCNTs. Wet cake dispersions in an aqueous environment of both dMWCNT formulations appeared black, homogenous, and uniform under high

magnification light microscopy at 10 mg/mL. Samples were characterized by scanning electron microscopy (SEM), transmission electron microscopy (TEM), Fourier-transform infrared spectroscopy (FTIR), thermogravimetric analysis (TGA), and zeta potential (ZP). By SEM, unprocessed MWCNTs formed large, micron-scale clusters of hundreds to thousands of aggregated tubes; these contrasted dMWCNTs and PEG-dMWCNTs, which appeared as individualized tubes having both tube ends clearly present with no detectable aggregation (Figure 1A). Whereas dMWCNTs and PEG-dMWCNTs appeared individual and clean (lacking brighter spots indicative of catalyst metal presence), raw MWCNTs appeared webbed, indicating extraneous contamination, and occasionally had bright spots indicating impurities (Figure 1A). Thus, even after drying for SEM imaging, dMWCNTs and PEG-dMWCNTs remained individualized, exhibiting their non-aggregative properties. TEM imaging of unprocessed MWCNT material revealed similarly large multi-micron-sized bundles l (Figure 1B). Following purification and detanglement, individual tubes, lacking large agglomerates, comprised the dMWCNT and PEG-dMWCNT samples (Figure 1B). Based on TEM measurements and mass balance equations, dMWCNTs and PEG-dMWCNTs are ~900 nm long with ~11 nm outer diameters, ~5 nm inner diameters, and 12 concentric tubes.

The FTIR spectrum of dMWCNTs was dominated by the architecture of carbon-carbon bonding (Figure 1C). Intense banding in the 1700-1500cm^{-1} range, peaking at 1561cm^{-1}, can be attributed to aromatic C=C structures, while peaks in the 3700-2700cm^{-1} range (3741cm^{-1}, 3445cm^{-1} and 2938cm^{-1}) attest to the presence of O-H groups in alcohol and carboxylic acid moieties. The strong shoulder in the 800-400cm^{-1} region (peaking at 477cm^{-1}) is associated with sp2 C-H bending in the aromatic structure of the carbon nanotubes. The spectrum of PEG-dMWCNTs confirms surface-functionalization with PEG, as demonstrated the broad shoulder in the 1300-1000cm^{-1} range (peaking at 1082cm^{-1}) associated with C-O bonds in the PEG structure, as well as the peak at 2920cm^{-1} representing alkoxy structures in the backbone of PEG. Thermogravimetric analysis further confirmed that bulk MWCNTs have a very low oxidation percentage (0.3334%) and high residuals (2.796%) (Figure 1D, dotted line), while, purified dMWCNTs (Figure 1D, solid line) had a much higher percent oxidation (2.22% wt/wt), lower residuals (0.2036% wt/wt) and a decomposition peak at 331.52°C. As expected, the % oxidation increased substantially in PEGylated dMWCNTs (to 9.712% wt/wt) while residuals increased slightly (to 0.6046% wt/wt) (Figure 1E, solid line). There was no change seen in peak temperature of decomposition (332.22°C), indicating the presence of bound PEG molecules. The density of oxygenated species on dMWCNTs was measured by micro-titration. We measured a density of 0.09 mmols/gram tubes for -COOH groups, or 0.95% wt., corresponding to ~2% weight oxidation. We determined an -OH density of 0.17 mmols/gram, or 0.34% wt., and 0.19% wt. of lactones. The bulk conductivity of dried, pressed mats measured 3 ohm-cm with a measured density of 0.32 g/cc. In total, these properties suggested that the dMWCNTs and PEG-dMWCNTs held promise for cell-based therapies.

In Vitro Toxicity Assays

Cytotoxicity of dMWCNTs and PEG-dMWCNTs was assessed in a variety of cell types (Figure 2A-C). dMWCNTs, although reasonably well tolerated at 0.01 mg/mL,

demonstrated a time- and dose-dependent inhibitory effect on survival of OPM2 myeloma cells while PEG-dMWCNTs were less cytotoxic, showing only toxicity at 1 mg/mL after 48-hours (Figure 2A). Similarly, human bone marrow-derived mesenchymal stem cells (hMSCs) (Figure 2B) and preadipocytes (3T3L1 cells) (Figure 3C) also showed greater toxicity response when exposed to dMWCNTs than PEG-dMWCNTs in a dose and time dependent-manner. LogEC50 values in hMSC's were the same between dMWCNT and PEG-dMWCNT's after 24 and 48 hour at 0.1011 mg/ml. LogEC50 values in 3T3L1 cells were also the same between dMWCNTs and PEG-dMWCNTs at 0.1085 mg/ml after 24 and 48 hours. Interestingly, by 2-way ANOVA, treatment concentration and type (dMWCNT or PEG-dMWCNT) had significant effects on survival for OPM2 and hMSCs at 24 and 48 hours, and 3T3L1 cells at 48 hours.

Next, we investigated if exposure to PEG-dMWCNTs induced chromosome instability by treating 3T3L1 cells with a dose range of PEG-dMWCNTs for 120 hours (Supplementary Figure 1). None of the PEG-dMWCNT concentrations tested induced chromosomal damage. As a comparison and positive control, we used mitomycin C to show that 3T3L1 cells have chromosomal aberrations when exposed to a genotoxic agent. This indicated that PEG-dMWCNTs do not induce structural chromosome instability and are not genotoxic. Lastly, we assessed morphological cell transformation through standard focus formation assays after 120 hours of treatment with PEG-dMWCNTs in HOS cells (Supplementary Table 1). We observed a low frequency of focus formation after chronic exposure to PEG-dMWCNTs (Supplementary Table 1), while the positive control (3MC) induced 10-fold more foci than the highest PEG-dMWCNT dose tested. Foci were further tested for anchorage independence by performing a soft agar colony-forming analysis. As seen in Supplementary Table 1, there was no difference in the average number of soft agar colonies between control cells (untreated) and foci derived from PEG-dMWCNT treated-cells. MCF7 cells were used as a positive control in the soft agar colony efficiency assay following published methods [27], Thus, *in vitro*, PEG-dMWCNTs appear safe for cell cultures.

In Vivo Tolerability and Biodistribution

To quantitatively assess clearance rates and biodistribution patterns in organs, PEG-dMWCNTs were tracked and quantified with Lu^{177} (see Supplementary methods). A single dose of 20 mg/kg (8 μCi/mouse) was administered via the tail vein and scintillation counting was performed on organs after sacrifice. Blood enzyme analysis demonstrated no significant effects of PEG-dMWCNTs on kidney or liver function (Supplementary Figure 2A-C). All mice tolerated the administration and no treatment-related weight loss or signs of toxicity were observed. Clearance of PEG-dMWCNTs occurred on the order of days to weeks and appeared to proceed through the reticuloendothelial system resulting in clearance via urine or feces (Supplementary Figure 2D). As the PEG-dMWCNTs began to clear from the blood, they moved into the liver, spleen, and bone. After 10 days, ~50% of the total dose remained in the liver, ~12% in the spleen, and ~10% in the bone (Supplementary Figure 2D-E). At 34 days, <38% of the initial dose remained in the liver, <8% in the spleen, and ~13% in the bone (Supplementary Figure 2D, E). The heart, muscles, and intestines all had >15% of the initial dose and initial dose per gram of tissue (Supplementary Figure 2D, E).

Formulation and Characterization of Bone-Targeted PEG-dMWCNTs

We next formulated PEG-dMWCNTs for organ-specific targeting by grafting a bisphosphonate, alendronate, onto the surface of Cy5-PEG-dMWCNTs to create fluorescent, bone-targeted dMWCNTs (BT-PEG-dMWCNTs). When Cy5-PEG-dMWCNTs and Cy5-BT-PEG-dMWCNTs were incubated with mouse bones *ex vivo*, only the BT-dMWCNTs remained associated with the bone surface following the washing steps, indicating successful attachment of functional bone-targeting moieties (Figure 3A) and quantified by fluorescence measurements (Figure 3B, C). SEM and TEM analysis of BT-PEG-dMWCNTs indicated an outer diameter of 10.74 nm ± 2.46 nm (SD) and an inner diameter of 4.959 nm ±1.07 nm (SD), n=15, with no morphological difference relative to dMWCNTs or PEG-dMWCNTs (Figure 3D, E). BT-PEG-dMWCNTs were also compared to PEG-dMWCNTs using FTIR, TGA, ZP and cell toxicity assays (Figure 4A-F). FTIR demonstrated alendronate surface-grafting where bands associated with phosphorus containing-moieties are prevalent in the 1400-1000cm^{-1} range (with peaks at 1385cm^{-1}, 1179cm^{-1}, 1127cm^{-1} and 1066cm^{-1}), while the secondary amine formed by functionalization to the dMWCNT surface is represented by bands at 1700-1500cm^{-1} range, with peaks at 1638cm^{-1} and 1582cm^{-1} (Figure 4A, B).

Similar stability profiles were observed between dMWCNT formulations (Figure 4C, D), where ZP measurements showed maximal stability after 20 mins of sonication and maintenance after 3 months in suspension (Figure 4C, D). Lastly, TGA analysis showed that BT-PEG-dMWCNTs were comparable to PEG-dMWCNTs in terms of residuals and % functionalization but showed a slight increase in their peak decomposition temperature from 332.22°C to 377.64°C, attributable to phosphate groups of alendronate (Table 1). There were also no differences in cell toxicity (Figure 4E, F), chromosomal aberration (Supplementary Figure 3) neoplastic transformation (Supplementary Table 2) or dispersability in aqueous environment resulting from the addition of alendronate to PEG-dMWCNTs.

In Vitro Drug Loading and Release, and In Vivo Pharmacokinetic (PK) Studies

PEG-dMWCNTs were loaded with doxorubicin (DOX) in order to develop a strategy for targeted therapeutic dosing in clinical applications. We hypothesized that the side effects of DOX on mice would be mitigated if DOX was loaded on PEG-dMWCNTs. DOX had high dMWCNT-binding capacity and was slowly released from PEG-dMWCNTs and BT-PEG-dMWCNTs (Figure 5). The mass ratio of DOX loading onto dMWCNTs was measured to be 35% wt/wt with a ~95% wt/wt loading efficiency (Figure 5A). Higher load mass ratios were achieved, but caused lower loading efficiency and 35% wt/wt loading was used in all further studies. Stoichiometrically, this indicates that 1 molecule of PEG-dMWCNT sequestered ~134,000 molecules of DOX. The high number of drug molecules per PEG-dMWCNT suggests that a low number of dMWCNTs (low dose) may be able to deliver an efficacious level of pharmacological agent. There was no difference in loading between bone-targeting and non-targeting PEG-dMWCNTs (Figure 5A).

To test *in vitro* drug release, we diluted DOX-loaded PEG-dMWCNTs and BT-PEG-dMWCNTs with PBS and measured release of DOX over time. We observed an initial burst of ~30% wt/wt after 8 hours, followed by a slow release profile with 51% wt/wt released

after 48 hours, with no differences between BT-PEG-dMWCNT and PEG-dMWCNT release profiles (Figure 5B). The slow off-rate suggests that dMWCNTs could alter the pharmacokinetic properties of DOX by releasing it slowly into the body, creating regions of high DOX concentration at sites where PEG-dMWCNTs are localized. DOX loading/unloading results, along with studies with other drugs and dyes (data not shown), indicate that PEG-dMWCNTs load and off-load cargo molecules in physiologically-relevant timeframes.

To investigate *in vivo* release, mice were treated with 3 mg/Kg of free DOX or an equivalent mass loaded into PEG-dMWCNTs (8.57 mg/kg). Blood serum DOX concentrations were monitored at regular time points. An altered pharmacokinetic profile, relative to free drug, was observed within the 3 hours following administration (Figure 5C). Initial plasma concentrations were lower for the rapidly-cleared free drug, suggesting a lower elimination rate for DOX loaded on PEG-dMWCNTs. PEG-dMWCNTs doubled the AUC parameter of DOX, indicating an enhanced systemic exposure window that should enhance drug action (Figure 5D). As both free and PEG-dMWCNT-loaded DOX entered tissues and began to clear the circulation after 3 hours, their plasma concentrations approached parity; this was expected after the results of the biodistribution study indicated that PEG-dMWCNTs clear from the blood in that same time frame. However, PEG-dMWCNTs did not necessarily alter DOX metabolism, only its distribution, thus the rates of clearance are not significantly altered and half-lives appear similar (Figure 5E). Given the high distribution of PEG-dMWCNTs into the liver after the first 24-48 hours, livers were assayed for DOX at the endpoint of the experiment. Concentrations of the active-form of DOX were doubled compared to the free DOX group (Figure 5F), suggesting that PEG-dMWCNTs do not alter DOX metabolism and potentially are more stable in the liver when loaded onto PEG-dMWCNTs. This pharmacokinetic study demonstrated that PEG-dMWCNTs can be used as a drug delivery agent *in vivo*, and that they can alter the pharmacokinetics and biodistribution of cargo.

DOX-loaded PEG-dMWCNTs and BT-PEG-dMWCNTs are Effective in vitro Against Burkitt's Lymphoma

To test the efficacy of doxorubicin (DOX)-loaded dMWCNTs *in vitro*, treated Raji.luc cells were treated with dMWCNTs, free DOX, DOX-loaded PEG-dMWCNTs, or DOX-loaded BT-PEG-dMWCNTs. Raji.luc cells were more sensitive to unloaded PEG-dMWCNTs than BT-PEG-dMWCNTs, at concentrations 0.1 and 1 mg/mL after 48 hours (Figure 6A). Drug loading studies were performed only with lower dose ranges of PEG-dMWCNTs and BT-PEG-dMWCNTs (ranging from 0.048 mg/mL to 0.00048 mg/mL PEG-dMWCNTs), to investigate changes in DOX toxicity when delivered in dMWCNTs (Figure 6B). DOX-loaded dMWCNTs Killed Raji.luc cells in a dose- and time-dependent manner (Figure 6B), and the EC50 was slightly increased, which is likely because of the slow off-rate of the drug from the surface of the tube (Figure 6B). At 24 hours, free DOX killed tumor cells more effectively than dMWCNT-loaded DOX *in vitro*, but differences between loaded and free drug were abrogated after 48 hours. We observed that doses as low as 0.046 mg/mL PEG-dMWCNTs and BT-PEG-dMWCNTs (corresponding to 25,000 nM DOX, the highest concentration point tested) also had a slight inhibitory effect on Raji.luc cells. This finding

suggested that Raji.luc cells may be susceptible to death via dMWCNTs alone, and this is consistent with a delayed drug release profile of DOX from the dMWCNTs. Overall, we saw effective *in vitro* DOX loading, release, and anti-tumor action using both PEG-dMWCNTs and BT-PEG-dMWCNTs.

DOX-loaded PEG-dMWCNTs and BT-PEG-dMWCNTs in an Orthotopic Model of Burkitt's Lymphoma

We next tested efficacy of DOX-loaded dMWCNTs *in vivo*. We hypothesized that the pharmacokinetic differences between free and dMWCNT-loaded DOX would induce differences in DOX efficacy in a lymphoma model, and that loading would decrease DOX-induced toxicity. As the Raji.luc model grows predominantly in the skeleton, we also hypothesized that BT-PEG-dMWCNTs would have greater anti-lymphoma effects versus the untargeted PEG-dMWCNTs. To test this, mice were inoculated with Raji.luc cells and treated with 5 mg/kg DOX as a free drug or loaded onto either PEG-dMWCNTs or BT-PEG-dMWCNTs. Body weights, bioluminescent imaging (BLI) data, and survival curve data were acquired and 14.29 mg/kg PEG-dMWCNTs were used for all PEG-dMWCNT groups, with empty PEG-dMWCNTs and "no-treatment" used as controls. The study was ended at day 45 when significance between groups was evident; any mice still alive were considered censored at this point for survival curve analysis.

The free DOX, PEG-dMWCNT-bound DOX, and BT-PEG-dMWCNT-bound DOX groups all showed significant decreases in tumor burden with whole mouse BLI versus the no-treatment control (Figure 7A). The unloaded PEG-dMWCNT group alone also showed decreased tumor burden versus the control (Figure 7A), which paralleled our *in vitro* data that showed PEG-dMWCNTs can have a direct anti-lymphoma effect after 48 hours. However, both types of DOX-loaded dMWCNTs and free DOX all significantly decreased tumor burdens compared to PEG-dMWCNTs alone. Tumor burden analysis also demonstrated that DOX-loaded BT-PEG-dMWCNTs and DOX-loaded PEG-dMWCNTs had a similar capacity to decrease tumor burden and equally effective to free DOX (Figure 7A). The aggressive DOX treatment used in the study may have masked any efficacy improvement in BLI that could have resulted from delivering DOX loaded on either PEG-dMWCNTs or BT-PEG-dMWCNTs relative to free DOX.

Survival data showed the median time to endpoint (TTE) for the non-treated control group was 33 days while all the treated groups presented a median TTE of 45 days. This was also reflected in significant survival curve difference using the Log-rank (Mantel-Cox) Test for control versus PEG-dMWCNTs alone ($p=0.00391$), control versus free DOX ($p=0.0074$), control versus DOX-loaded PEG-dMWCNTs ($p=0.0001$), and control versus DOX-loaded BT-PEG-dMWCNTs ($p=0.0001$) (Figure 7B). The DOX-loaded dMWCNT groups both achieved a 100% survival rate until the end of the study on day 45. The group receiving free DOX incurred two deaths on days 29 and 31, which we believe were related to DOX toxicity rather than tumor, due to the low mouse BLI signal and absence of paralysis indications. Furthermore, the free DOX group demonstrated severe signs of treatment-related toxicity as evidenced by 15% weight loss by day 15 (Figure 7C), while DOX-loaded dMWCNT groups had only moderate weight loss. Statistical comparisons of body weight loss showed no

significance between groups before day 8. On day 8, the free DOX group had significant weight loss compared to the control group, and no other treatments caused significant or noticeable weight loss (Supplementary Table 3; Figure 7C). From day 11 onward, all groups showed significant weight loss as compared to the control group, except for the PEG-dMWCNT groups on day 25 and 15, with the greatest weight loss consistently observed in the free DOX group (Supplementary Table 3; Figure 7C). Interestingly, BT and non-targeted PEG-dMWCNTs appeared to be equally effective in terms of reducing mouse weight loss, decreasing tumor burden, and delaying death. In sum, PEG-dMWCNTs and BT-PEG-dMWCNTs both proved safe and effective at decreasing DOX toxicity and killing lymphoma cells *in vivo*. These novel dMWCNTs thus hold great potential for being used as a nanomedicine and reducing toxicity for patients in the future.

Discussion

Herein we developed and characterized novel PEG-dMWCNTs that were customized with robust binding of doxorubicin, Lu^{177}, Cy5, PEG, and targeting molecules (alendronate). We determined their utility as drug delivery molecules, confirmed cellular compatibility and nontoxicity, and performed *in vivo* studies to address toxicity, clearance, drug release, and anti-cancer efficacy. Our studies suggest that these PEG-dMWCNTs overcome many of the de-bundling and stability challenges that often serve as obstacles to CNT translation [14], and hold great promise as a novel, safe drug delivery system for hematological malignancies.

Our pharmacokinetics study of DOX-loaded PEG-dMWCNTs indicated that the effective concentration of DOX over time is two-fold higher in the serum when loaded on PEG-dMWCNT, and loaded DOX is more than twice as abundant as the free-form in the liver after 48 hours. These data indicate that, loading of DOX onto PEG-dMWCNTs may improve clearance and biodistribution properties and suggests a more stable drug-delivery system *in vivo*. It appears that when PEG-dMWCNTs localize in the bone, liver, spleen, and other organs, DOX is concentrated in those areas, rather than distributing systemically. In addition, when DOX was administered by loaded dMWCNTs, treatment-related weight loss was eliminated in a Burkitt's lymphoma model. Thus, PEG-dMWCNT drug delivery enabled equal efficacy with lowered side effects versus free drug. Minimal difference between DOX-loaded, BT-PEG-dMWCNTs and non-targeted PEG-dMWCNTs was observed and both treatments elicited similar responses to free DOX, likely because the DOX concentration used was too high to effectively resolve differences between groups [28,29]. Further animal studies with lowered DOX administration doses are warranted to elucidate any potential increase in efficacy with BT-PEG-dMWCNTs. Thus, our data indicate that dMWCNTs hold great potential for delivering therapeutics without causing toxicity and would likely decrease off-target toxicities due to systemic, rather than targeted or slow release, drug delivery for chemotherapies. Other groups have found similar outcomes with hepatocellular carcinoma, demonstrating an ability to load DOX into carbon nanotubes and indicating efficacy along with negligible *in vivo* toxicity. For example, Ji et al. developed chitosan-modified single walled CNTs, and used these to deliver folic acid and DOX for selective killing of hepatocellular carcinoma [30], and Zhao et al. also developed PEG-MWCNTs and found these to be non-toxic and capable of delivering DOX to a

hepatocellular carcinoma model *in vivo* [31]. Due to the strong liver targeting of our tubes, we also propose future work investigating liver hepatocellular carcinoma.

In summary, our studies report the first design of engineered bone-targeting, discrete, multiwalled CNTs used in a bone cancer model. This novel technology holds promise for bone-targeting drug delivery for diseases of the bone and bone marrow. We found that dMWCNTs can be tuned to load many therapeutically relevant biomolecules, such as peptides, proteins, siRNA, small molecules, targeting moieties, or fluorophores (not all shown here), either by passive diffusion or covalent bonding. dMWCNTs represent a very promising platform for drug delivery and organ-specific targeting, and the effects of dMWCNT-loading on biodistribution of therapeutic molecules were exemplified by bone-specific delivery in our Burkitt's lymphoma model. Future studies are aimed surface-grafting proteins and other biomolecular components to dMWCNTs in order more-finely control biodistribution and increase specific targeting of organs and tissues. Other interesting future directions include further characterizing dMWCNTs using atomic force microscopy (AFM), characterizing *in vivo* hemolytic toxicity and further characterization of chemical or physical functionalization efficiencies. Multi-functional composites may also be developed by combining dMWCNTs with other materials to further regulate drug release in the form of circulating particles or nanostructured-implants. Due to the versatility and fascinating properties of these materials, their most important potential biomedical applications may remain to be discovered and exploited.

Supplementary Material

Refer to Web version on PubMed Central for supplementary material.

Acknowledgements

hMSCs were obtained from the MMC BioBank. We thank Heather Fairfield and Anna Sitarski for their contributions to this project. We thank Dr. Cliff Rosen and Dr. Don St. Germain for their support of this work and this collaboration.

Disclosure Statement: Aaron W. Tasset, Paul Everill, and Milos Marinkovic are employees or contractors of BioPact LLC. Michaela Reagan receives research funding from BioPact LLC. All other authors have nothing to disclose. Funding was supplied by the National Institute of General Medical Sciences NIH P30 GM106391, Phase III COBRE in Progenitor Cells, NIH P30GM103392, Phase III COBRE in Vascular Biology, and the NIH/NIGMS (P20GM121301). The authors' work is also supported by start-up funds from the Maine Medical Center Research Institute and the American Cancer Society (Research Grant #IRG-16-191-33). This work was also partially supported by the NIH/NIAMS P30AR066261. The content is solely the responsibility of the authors and does not necessarily represent the official views of the NIH.

References

1. Iijima S. Helical microtubules of graphitic carbon. Lett. To Nat 353, 737–740 (1991).
2. Teradal NL, Jelinek R. Carbon Nanomaterials in Biological Studies and Biomedicine. Adv. Healthc. Mater , 1700574 (2017).
3. Lalwani G, Patel SC, Sitharaman B. Two- and Three-Dimensional All-Carbon Nanomaterial Assemblies for Tissue Engineering and Regenerative Medicine. Ann. Biomed. Eng 44(6), 1–16 (2016). [PubMed: 26620776]
4. Arun S, Kanagaraj S. Mechanical characterization and validation of poly (methyl methacrylate)/ multi walled carbon nanotube composite for the polycentric knee joint. J. Mech. Behav. Biomed. Mater 50(10 2015), 33–42 (2015). [PubMed: 26099200]

5. Re F, Moresco R, Masserini M. Nanoparticles for neuroimaging. J. Phys. D. Appl. Phys 45(7), 073001 (2012).
6. Singh S, Mehra NK, Jain NK. Development and Characterization of the Paclitaxel loaded Riboflavin and Thiamine Conjugated Carbon Nanotubes for Cancer Treatment. Pharm. Res 33(7), 1769–1781 (2016). [PubMed: 27091032]
7. Dong X, Sun Z, Wang X, Zhu D, Liu L, Leng X. Simultaneous monitoring of the drug release and antitumor effect of a novel drug delivery system-MWCNTs/DOX/TC. Drug Deliv. 24(1), 143–151 (2017). [PubMed: 28156171]
8. Malarkey EB, Parpura V. Carbon Nanotubes in Neuroscience. In: Acta neurochirurgica. Supplement. , 337–341 (2010). [PubMed: 19812974]
9. Kobayashi N, Izumi H, Morimoto Y. Review of toxicity studies of carbon nanotubes. J. Occup. Health (2017).
10. Lam C, James J, McCluskey R, Arepalli S, Hunter R. A review of carbon nanotube toxicity and assessment of potential occupational and environmental health risks. Crit. Rev. Toxicol 36(3), 189–217 (2006). [PubMed: 16686422]
11. Sharifi S, Behzadi S, Laurent S, Forrest ML, Stroeve P, Mahmoudi M. Toxicity of nanomaterials. Vet. Toxicol 41, 2323–2343 (2012).
12. Ali-Boucetta H, Al-Jamal KT, McCarthy D, Prato M, Bianco A, Kostarelos K. Multiwalled carbon nanotube–doxorubicin supramolecular complexes for cancer therapeutics. Chem. Commun (4), 459–61 (2008).
13. Zhang X, Meng L, Lu Q, Fei Z, Dyson PJ. Targeted delivery and controlled release of doxorubicin to cancer cells using modified single wall carbon nanotubes. Biomaterials. 30(30), 6041–7 (2009). [PubMed: 19643474]
14. Cheng KT, McDevitt MR, Scheinberg DA. Single-walled carbon nanotubes-(111)In-1,4,7,10-tetraazacyclododecane-N,N',N",N"'-tetraacetic acid-rituximab. National Center for Biotechnology Information (US).
15. Marches R, Chakravarty P, Musselman IH, Bajaj P, Azad RN, Pantano P et al. Specific thermal ablation of tumor cells using single-walled carbon nanotubes targeted by covalently-coupled monoclonal antibodies. Int. J. Cancer 125(12), 2970–2977 (2009). [PubMed: 19536775]
16. Taghdisi SM, Lavaee P, Ramezani M, Abnous K. Reversible Targeting and controlled release delivery of daunorubicin to cancer cells by aptamer-wrapped carbon nanotubes. Eur. J. Pharm. Biopharm 77(2), 200–206 (2011). [PubMed: 21168488]
17. Tavakolifard S, Biazar E. Nano Biomed Eng Modification of Carbon Nanotubes as an Effective Solution for Cancer Therapy. 8(3), 144–160 (2016).
18. Dumortier H, Lacotte S, Pastorin G, Marega R, Wu W, Bonifazi D, et al. Functionalized carbon nanotubes are non-cytotoxic and preserve the functionality of primary immune cells. Nano Lett. 6(7), 1522–8 (2006). [PubMed: 16834443]
19. Lee JJ, Saiful Yazan L, Che Abdullah CA. A review on current nanomaterials and their drug conjugate for targeted breast cancer treatment. Int. J. Nanomedicine 12, 2373–2384 (2017). [PubMed: 28392694]
20. Sayes CM, Liang F, Hudson JL, Mendez J, Guo W, Beach JM, et al. Functionalization density dependence of single-walled carbon nanotubes cytotoxicity in vitro. Toxicol. Lett 161(2), 135–42 (2006). [PubMed: 16229976]
21. Huang YY, Terentjev EM. Dispersion of carbon nanotubes: Mixing, sonication, stabilization, and composite properties. Polymers (Basel). 4(1), 275–295 (2012).
22. Swogger SW, Everill P, Dubey DP, Sugumaran N. Discrete carbon nanotubes increase lead acid battery charge acceptance and performance. J. Power Sources 261, 55–63 (2014).
23. Sugumaran N, Everill P, Swogger SW, Dubey DP. Lead acid battery performance and cycle life increased through addition of discrete carbon nanotubes to both electrodes. J. Power Sources 279, 281–293 (2015).
24. Swoger KW, Bosnyak C. Creating molecular rebar from multi-wall carbon nanotubes. In: Annual Technical Conference , 448–451 (2002).

25. Peddini SK, Bosniak CP, Henderson NM, Ellison CJ, Paul DR. Nanocomposites from styrene-butadiene rubber (SBR) and multiwall carbon nanotubes (MWCNT) part 1: Morphology and rheology. Polymer (Guildf). 55(1), 258–270 (2014).
26. Peddini SK, Bosnyak CP, Henderson NM, Ellison CJ, Paul DR. Nanocomposites from styrene-butadiene rubber (SBR) and multiwall carbon nanotubes (MWCNT) part 2: Mechanical properties. Polym. (United Kingdom) 56, 443–451 (2015).
27. Schiavano GF, De Santi M, Brandi G, Fanelli M, Bucchini A, Giamperi L, et al. Inhibition of Breast Cancer Cell Proliferation and In Vitro Tumorigenesis by a New Red Apple Cultivar. PLoS One [Internet]. 10(8),e0135840(2015). Available from :http://dx.plos.org/10.1371/journal.pone.0135840. [PubMed: 26284516]
28. Allen TM, Mumbengegwi DR, Charrois GJR. Anti-CD19-targeted liposomal doxorubicin improves the therapeutic efficacy in murine B-cell lymphoma and ameliorates the toxicity of liposomes with varying drug release rates. Clin. Cancer Res [Internet]. 11(9), 3567–73 (2005). Available from: http://www.ncbi.nlm.nih.gov/pubmed/15867261. [PubMed: 15867261]
29. Lopes de Menezes DE, Pilarski LM, Allen TM. In vitro and in vivo targeting of immunoliposomal doxorubicin to human B-cell lymphoma. Cancer Res. [Internet]. 58(15), 3320–30 (1998). Available from: http://www.ncbi.nlm.nih.gov/pubmed/9699662. [PubMed: 9699662]
30. Ji Z, Lin G, Lu Q, Meng L, Shen X, Dong L, et al. Targeted therapy of SMMC-7721 liver cancer in vitro and in vivo with carbon nanotubes based drug delivery system. J. Colloid Interface Sci 365(1), 143–9 (2012). [PubMed: 21974923]
31. Zhao X, Tian K, Zhou T, Jia X, Li J, Liu P. PEGylated multi-walled carbon nanotubes as versatile vector for tumor-specific intracellular triggered release with enhanced anti-cancer efficiency: Optimization of length and PEGylation degree. Colloids Surf. B. Biointerfaces. (2018).
32. Fairfield H, Falank C, Harris E, Demambro V, McDonald M, Pettitt JA, et al. The skeletal cell-derived molecule sclerostin drives bone marrow adipogenesis. J. Cell. Physiol 233(2), 1156–1167 (2018). [PubMed: 28460416]
33. Swami A, Reagan MR, Basto P, Mishima Y, Kamaly N, Glavey S, et al. Engineered nanomedicine for myeloma and bone microenvironment targeting. Proc. Natl. Acad. Sci. U. S. A [Internet]. 111(28), 10287–92 (2014). [PubMed: 24982170]
34. McDonald MM, Reagan MR, Youlten SE, Mohaney ST, Seckinger A, Terry RL, et al. Inhibiting the osteocyte specific protein sclerostin increases bone mass and fracture resistance in multiple myeloma. Blood. , blood-2017-03-773341 (2017).
35. LaCerte C, Xie H, Aboueissa A-M, Wise JP. Particulate depleted uranium is cytotoxic and clastogenic to human lung epithelial cells. Mutat. Res. Toxicol. Environ. Mutagen [Internet]. 697(1–2),33–37 (2010).Available from: http://www.ncbi.nlm.nih.gov/pubmed/20172046.
36. Wise JP, Wise SS, Little JE. The cytotoxicity and genotoxicity of particulate and soluble hexavalent chromium in human lung cells. Mutat. Res. Toxicol. Environ. Mutagen [Internet]. 517(1–2),221–229(2002).Available from: http://linkinghub.elsevier.com/retrieve/pii/S1383571802000712.
37. Hernandez-Ilizaliturri FJ, Jupudy V, Ostberg J, Oflazoglu E, Huberman A, Repasky E, et al. Neutrophils contribute to the biological antitumor activity of rituximab in a non-Hodgkin's lymphoma severe combined immunodeficiency mouse model. Clin. Cancer Res 9(16 Pt 1), 5866–73 (2003). [PubMed: 14676108]

Highlights:

- Newly-developed, discrete multi-walled CNTs (dMWCNTs) are de-aggregated, uniform, pure, and stable.
- dMWCNTs were PEGylated to form PEG-dMWCNTs, and conjugated with alendronate to create bone targeting BT-PEG-dMWCNTs, which were all well tolerated *in vivo*.
- PEG-dMWCNTs and BT-PEG-dMWCNTs altered drug pharmacokinetics, showing their potential as a nanomedicine.
- PEG-dMWCNTs were successfully loaded with doxorubicin and decreased tumor burden in a mouse model of Burkitt's lymphoma similarly to free drug.
- PEG-dMWCNTs reduced doxorubicin (DOX) side effects in a mouse lymphoma model.

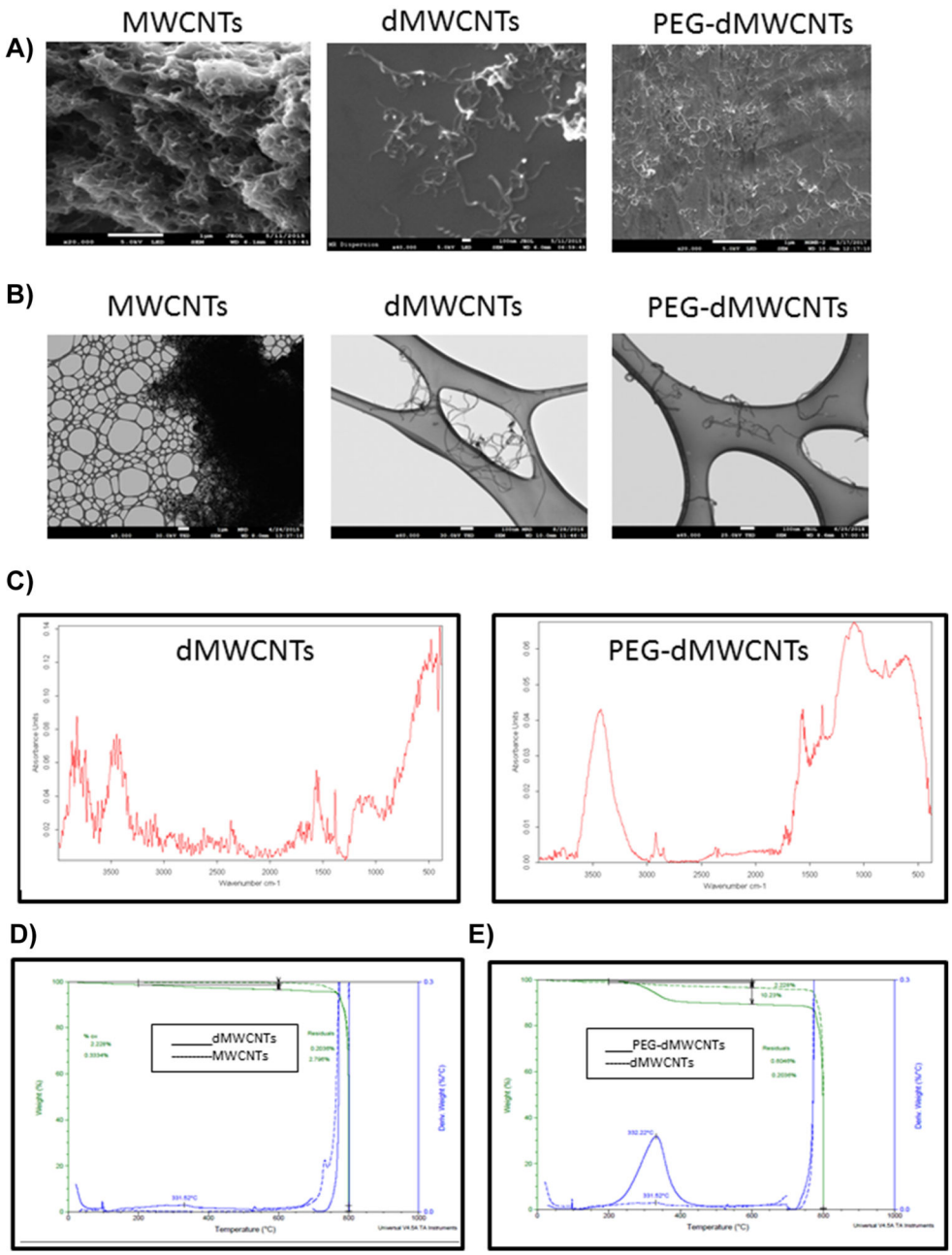

Figure 1: Physical Characterization of dMWCNTs.

A) Representative SEM micrographs of entangled CNTs aggregated tubes and individualized dMWCNTs and PEG-dMWCNTs are discrete and substantially free of contaminants (silicon wafer seen in backdrop). B) TEM analysis proves they have an outer diameter of 10.74 nm +/− 2.46 (SD) nm and an inner diameter of 4.959 nm +/−1.07 (SD). C) Molecular spectral properties using FTIR of dMWCNTs and functionalized PEG-dMWCNTs. D) TGA comparison between CNTs and dMWCNTs show an increase in oxidative functionalization and removal of metal catalyst during the cleaning process to yield dMWCNTs from CNTs E) TGA comparison between dMWCNTs and PEG-

dMWCNTs show an increase in functionalization due to the presence of PEG covalently attached to the surface.

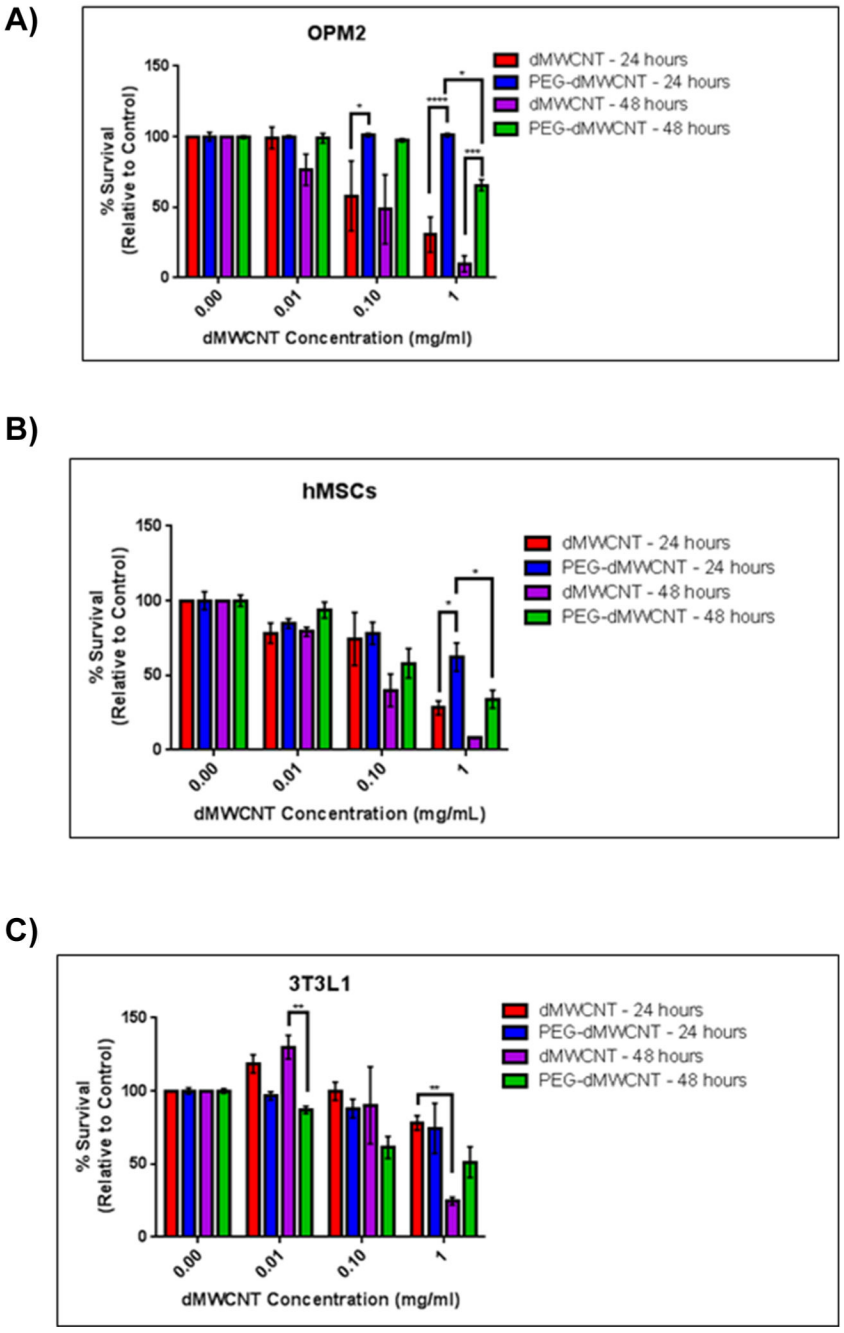

Figure 2: Cytotoxicity Profiles of dMWCNTs vs PEG-dMWCNTs.

Cytotoxicity assay comparing multiple cell types over a 24 and 48-hour treatment period with various doses of dMWCNTs and PEG-dMWCNTs (A) OPM2, (B) hMSCs, (C) 3T3L1 cells. Statistics were done using 2-way ANOVA with Sidak's multiple comparisons test at 24 and 48 hours for each cell line, n=4-6.

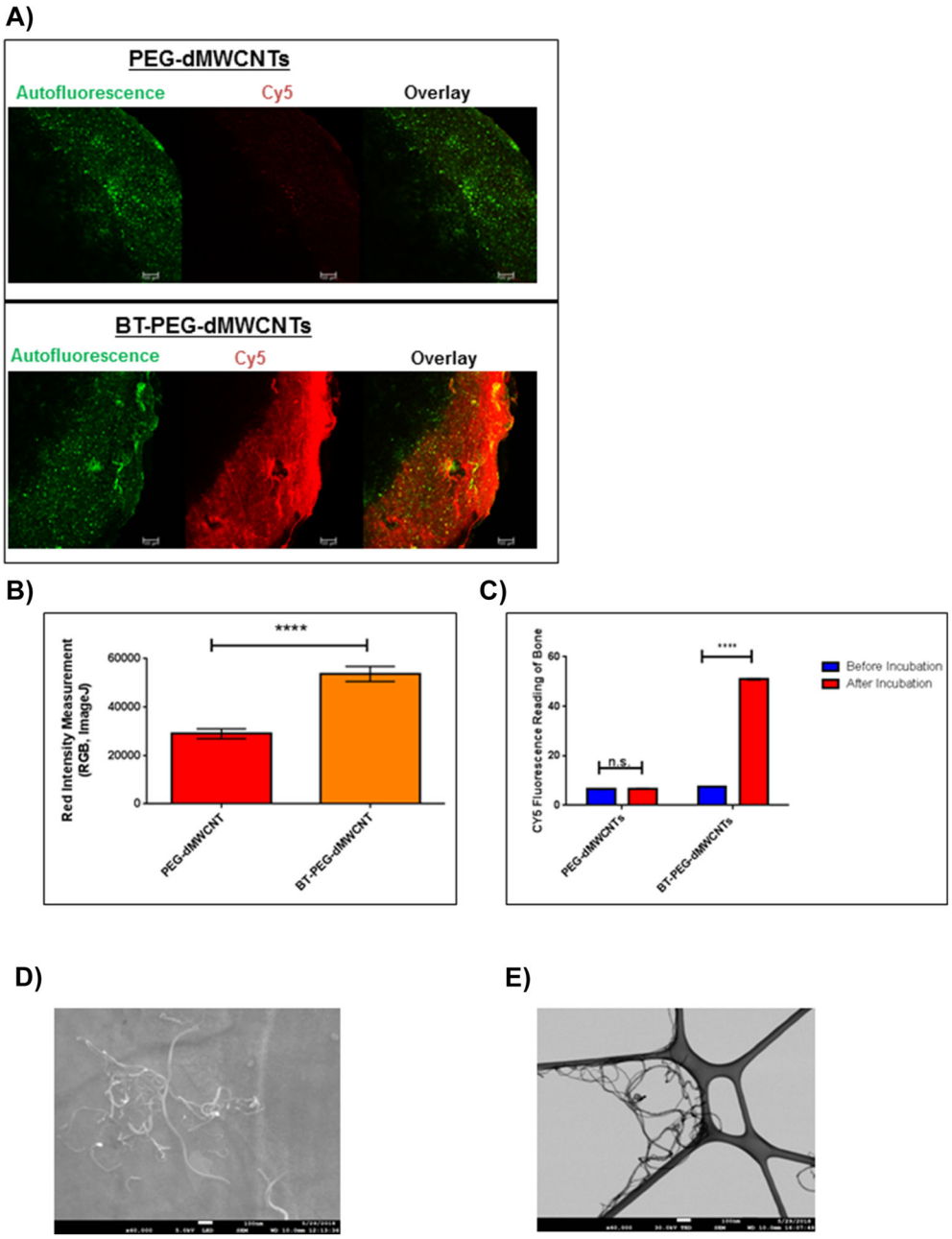

Figure 3: Development of BT-PEG-dMWCNTs.

A) Fluorescent imaging of *ex vivo* bones samples in which CY5-PEG-dMWCNTs and BT-CY5-PEG-dMWCNTs were incubated with mouse calvarias bone. Scale bar = 100μm. B) Quantification of the *ex vivo* BT-PEG-dMWCNT binding affinity at 2 hours using RGB (red, green blue) intensity measurements on ImageJ. C) Cy5 fluorescence reading of bone after PEG-dMWCNT and BT-PEG-dMWCNT incubation with bone autofluorescence subtracted out. Data are plotted as mean ± SEM. Statistical significance evaluated with Student's T-tests where **** represents $p<0.0001$. D) SEM of BT-PEG-dMWCNTs showed that the tubes maintained their individuality following attachment of alendronate. E) TEM of BT-PEG-dMWCNTs showed no distinguishable difference between PEG-dMWCNTs.

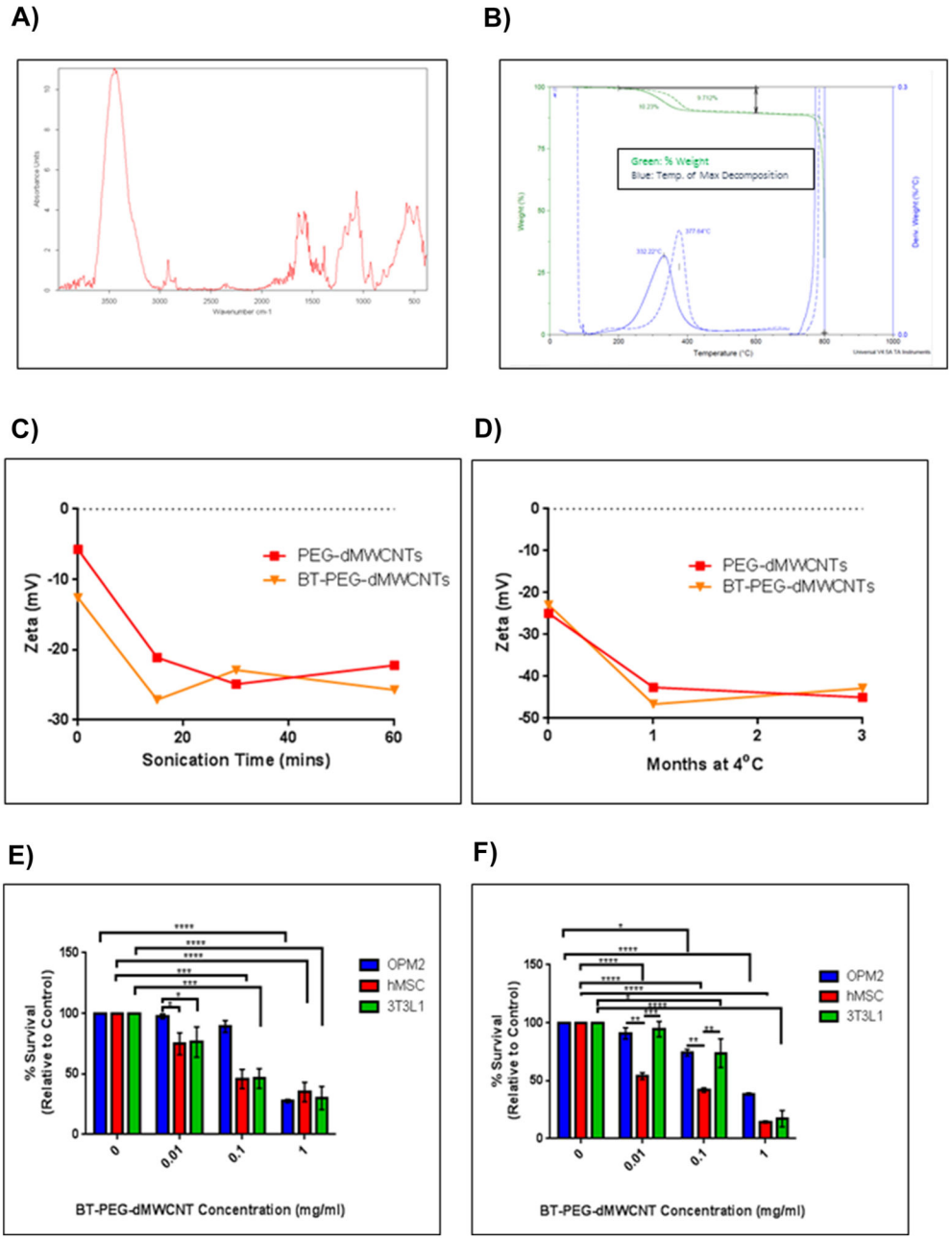

Figure 4. Characterization of BT-PEG-dMWCNTs.

Surface functionalization of alendronate by FTIR (A), TGA (B), and stability studies (C-D) of bone targeted PEG-dMWCNTs. E) Cell toxicity of BT-PEG-dMWCNTs in 3 cell types after 24 hours (E) and 48 hours (F) showed similar trends with more toxicity after 48 hours. Statistics were done using 2-way ANOVA with Sidak's multiple comparisons test at 24 and 48 hours for each cell line, n=3.

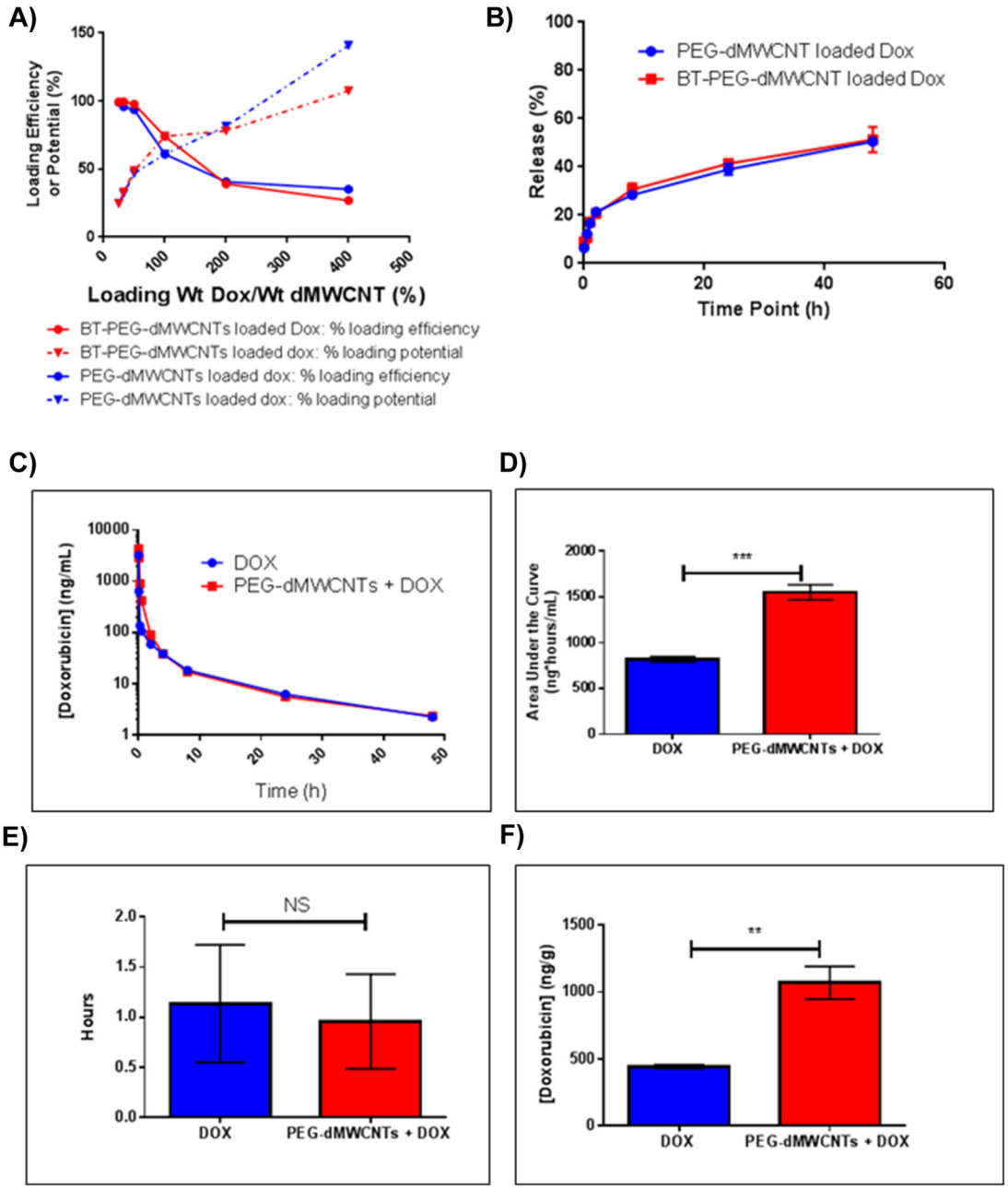

Figure 5: Loading and Release Properties of PEG-dMWCNTs and BT-PEG-dMWCNTs.

A) DOX loading efficacy and potential curves indicate PEG-dMWCNT saturation is 35% wt/wt with higher ratios leaving some DOX remaining unbound. B) Percent of Maximum Adjusted DOX Fluorescence showing off-rate analysis as an initial fast release through ~4 hours and a longer release over days. There is no difference between PEG-dMWCNTs and BT-PEG-dMWCNTs DOX release rate. C-F) *In Vivo* Pharmacokinetic Comparison of Free DOX vs. PEG-dMWCNT-Loaded DOX. C) Curve fit of blood serum [DOX] data over a 48h period from mice. PEG-dMWCNT-loaded DOX remained higher in the crucial first hours of circulation and both curves eventually plateau similarly. D) Area Under the Curve (AUC) calculation shows a doubling of the mouse's exposure to DOX when PEG-dMWCNT-

loaded. E) Calculated half-lives do not show a difference between free DOX and PEG-dMWCNT-DOX and indicates that Free DOX or DOX released from PEG-dMWCNTs are cleared and metabolized similarly. F)Liver DOX concentrations. Data are plotted as mean ± SEM. Statistically significance was evaluated with Student's T-tests where: **, p=0.0069; ***, p=0.0011.

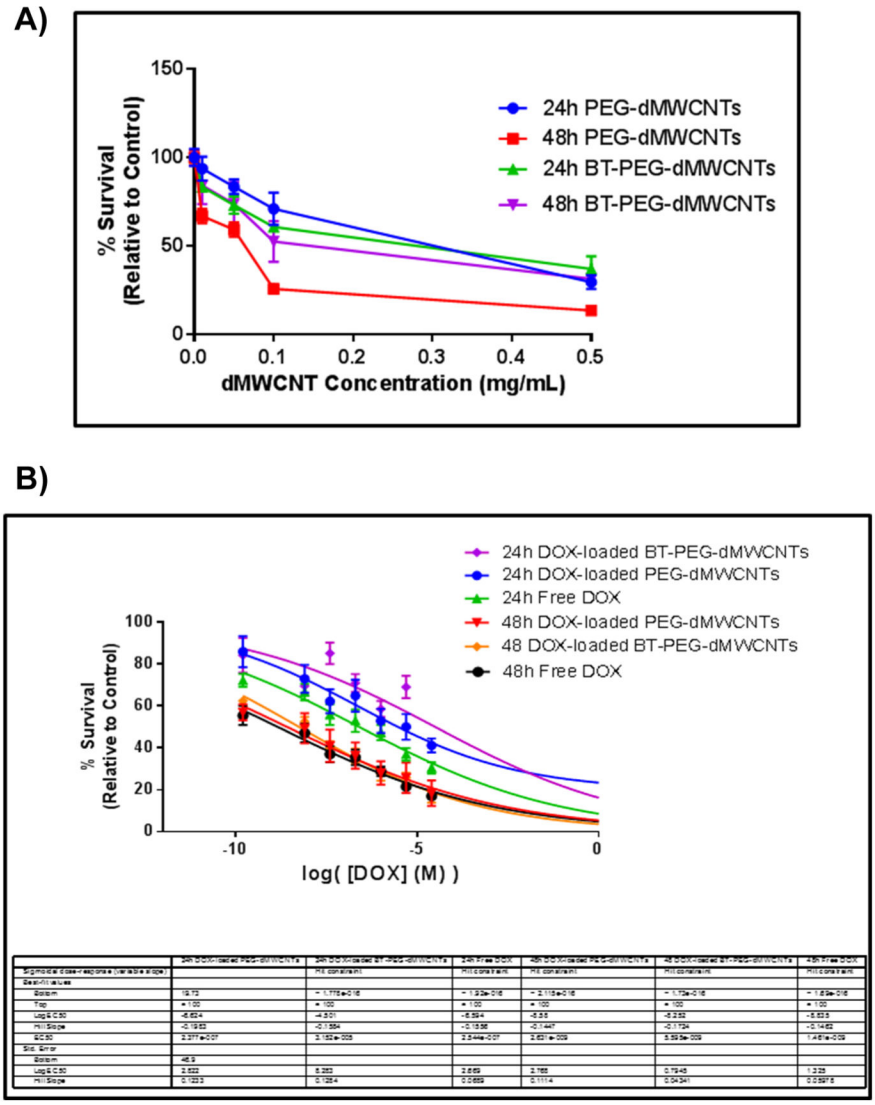

Figure 6: *In Vitro* Efficacy of DOX loaded dMWCNTs in Raji.luc cells.

A) Raji.luc cell survival assay reveals cell death in concentration-dependent manner in response to PEG-dMWCNTs and BT-PEG-dMWCNTs after 24 and 48 hours. 2-way ANOVA and Dunnett's multiple comparison test was done at each concentration for each time point with significance indicated with * ($p>0.05$) compared to control. B) Raji.luc cell survival assay reveals cell death in concentration- and time-dependent manner in response to DOX-loaded PEG-dMWCNTs, DOX-loaded BT-PEG-dMWCNTs and free DOX after 24 and 48 hours. Data is represented as mean ± SEM, n=12.

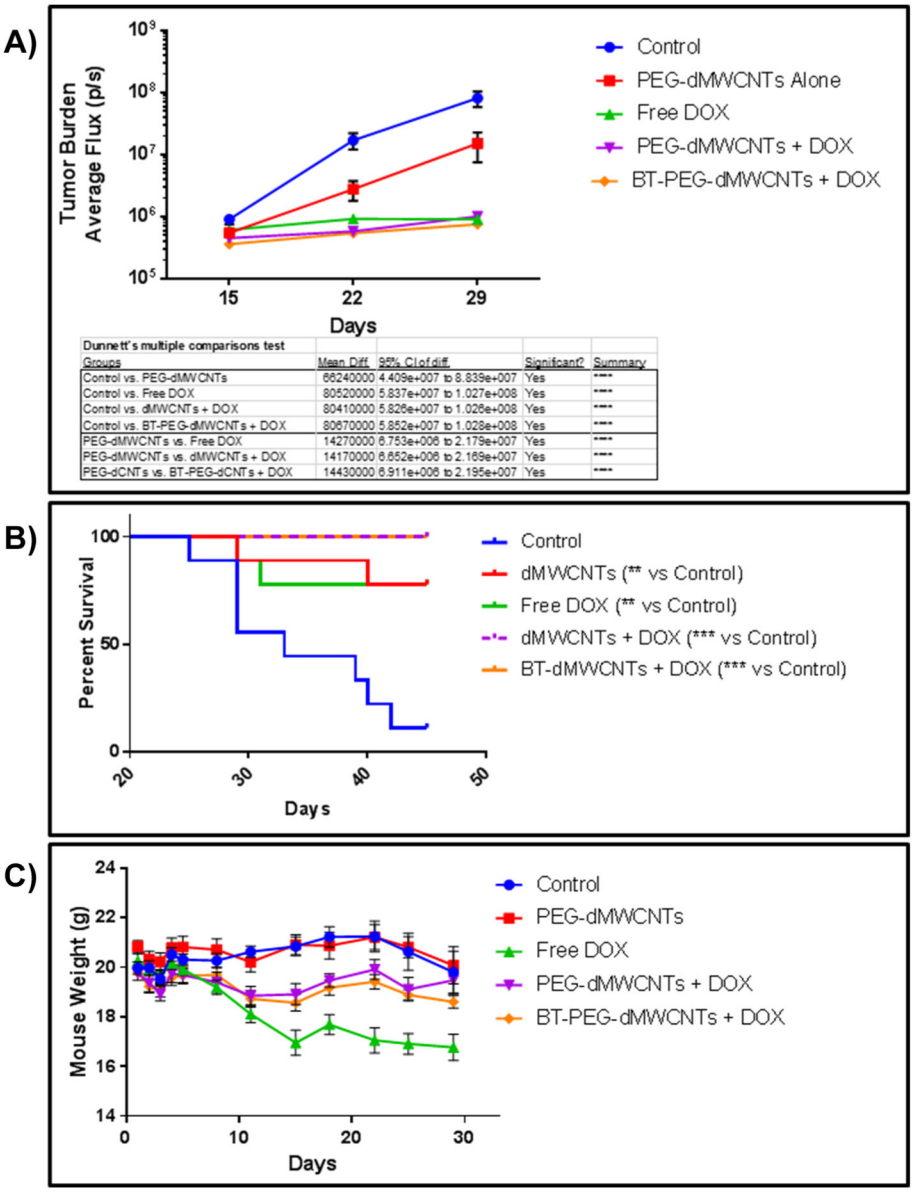

Dunnett's multiple comparisons test

Groups	Mean Diff.	95% CI of diff.	Significant?	Summary
Control vs. PEG-dMWCNTs	66240000	4.409e+007 to 8.839e+007	Yes	****
Control vs. Free DOX	80520000	5.837e+007 to 1.027e+008	Yes	****
Control vs. dMWCNTs + DOX	80410000	5.826e+007 to 1.026e+008	Yes	****
Control vs. BT-PEG-dMWCNTs + DOX	80670000	5.852e+007 to 1.028e+008	Yes	****
PEG-dMWCNTs vs. Free DOX	14270000	6.753e+006 to 2.179e+007	Yes	****
PEG-dMWCNTs vs. dMWCNTs + DOX	14170000	6.652e+006 to 2.169e+007	Yes	****
PEG-dCNTs vs. BT-PEG-dCNTs + DOX	14430000	6.911e+006 to 2.195e+007	Yes	****

Figure 7: Treatment of Burkett's Lymphoma with PEG-dMWCNT-Loaded and BT-PEG-dMWCNT-Loaded Doxorubicin.

A) BLI indicates a near complete abrogation of the tumor population in DOX and PEG-dMWCNT-loaded DOX groups and a decrease in tumor burden with PEG-dMWCNTs alone. B) Kaplan-Meier curve analysis showed a near total loss of control animals over the 45-d study but an increase in survival with free DOX, PEG-dMWCNT, PEG-dMWCNT-DOX, and BT-PEG-dMWCNT-DOX groups. Two mice were lost from the free DOX group due to treatment side effects; no animals were lost from either PEG-dMWCNT-loaded DOX group. C) DOX elicits a near 15% decrease in animal weight over 15 d, which was eliminated when DOX was dMWCNT loaded (see Table 2 for statistics). Data are plotted as mean ± SEM.

Table 1:

TGA Data.

TGA comparison between all CNTs and dMWCNTs shows % functionalization, residuals and temperature of maximum decomposition. CNTs originally contained high amounts of residual metal catalyst that are removed during the process to make dMWCNTs. The process to make dMWCNTs also increases the oxidative functionalization from 0.3334% (w/w) to 2.228% (w/w). Successful functionalization of dMWCNTs with PEG is indicated by the increase in % functionalization (determined by weight loss between 200 and 600°C) originating from the ether bonds of PEG. Successful attachment of the BT agent is indicated by the shift in temperature of maximum decomposition from 332.22 to 377.64, most likely originating from the presence of phosphate groups found on the BT agent.

	MWCNTs	dMWCNTs	PEG-dMWCNTs	BT-PEG-dMWCNTs
% Functionalization (w/w)	0.3334	2.228	10.23	9.712
Residuals % (w/w)	2.796	0.2036	0.6047	0.6274
Temperature of Max Degradation (deg C)	NA	331.52	332.22	377.64